

Measurement of T_{20} in Elastic Electron-Deuteron Scattering

M. Bouwhuis,¹ R. Alarcon,² T. Botto,¹ J. F. J. van den Brand,^{1,3} H. J. Bulten,³ S. Dolfini,² R. Ent,^{5,6} M. Ferro-Luzzi,¹ D. W. Higinbotham,⁸ C. W. de Jager,^{1,5,8} J. Lang,⁷ D. J. J. de Lange,¹ N. Papadakis,¹ I. Passchier,¹ H. R. Poolman,¹ E. Six,² J. J. M. Steijger,¹ N. Vodinas,¹ H. de Vries,¹ and Z.-L. Zhou⁴

¹*Nationaal Instituut voor Kernfysica en Hoge-Energie Fysica, P.O. Box 41882, 1009 DB Amsterdam, The Netherlands*

²*Department of Physics, Arizona State University, Tempe, Arizona 85287*

³*Department of Physics and Astronomy, Vrije Universiteit, 1081 HV Amsterdam, The Netherlands*

⁴*Department of Physics, University of Wisconsin, Madison, Wisconsin 53706*

⁵*Thomas Jefferson National Accelerator Facility, Newport News, Virginia 23606*

⁶*Department of Physics, Hampton University, Hampton, Virginia 23668*

⁷*Institute für Teilchenphysik, Eidgenössische Technische Hochschule, CH-8093 Zürich, Switzerland*

⁸*Department of Physics, University of Virginia, Charlottesville, Virginia 22901*

(Received 5 October 1998)

We report on a measurement of the tensor analyzing power T_{20} in elastic electron-deuteron scattering in the range of four-momentum transfer from 1.8 to 3.2 fm⁻¹. Electrons of 704 MeV were scattered from a polarized deuterium internal target. The tensor polarization of the deuterium nuclei was determined with an ion-extraction system, allowing an absolute measurement of T_{20} . The data are described well by a nonrelativistic calculation that includes the effects of meson-exchange currents. [S0031-9007(99)09127-9]

PACS numbers: 25.30.Bf, 13.40.Gp, 21.45.+v, 24.70.+s

The deuteron, as the simplest nucleus, serves as a sensitive testing ground for a variety of nuclear models (non-relativistic [1,2], fully covariant [3,4]). The charge and current distributions inside the nucleus can be probed with elastic electron scattering at intermediate energies. Elastic electron scattering off the spin-1 deuteron is completely described in terms of three electromagnetic form factors: the charge monopole G_C , the magnetic dipole G_M , and the charge quadrupole G_Q . Measurements of the unpolarized cross section yield the structure functions $A(G_C, G_M, G_Q)$ and $B(G_M)$. All three form factors can be separated, when either the tensor analyzing power T_{20} or the recoil deuteron tensor polarization t_{20} is also determined

[5]. The observables T_{20} and t_{20} contain an interference between G_C and G_Q and are thus sensitive to the effects of short-range and tensor correlations in the ground-state wave function of the deuteron. A large body of data is available for A and B for values of the four-momentum transfer Q of up to 12 fm⁻¹, while T_{20} has been measured up to 3.6 fm⁻¹ [6], albeit with limited accuracy, and t_{20} up to 4.6 fm⁻¹ [7]. In this paper absolute measurements with a small systematic error are presented on the analyzing power T_{20} in the $^2\text{H}(e, e'd)$ reaction for Q values between 1.8 and 3.2 fm⁻¹.

The cross section for elastic electron-deuteron scattering with unpolarized electrons and tensor-polarized deuterium nuclei can be expressed as [5]

$$\sigma = \sigma_0 \left[1 + \frac{A_d^T P_{zz}}{\sqrt{2}} \right], \quad \text{with } A_d^T = \sum_{i=0}^2 d_{2i} T_{2i} \quad \text{and} \quad (1)$$

$$d_{20} = \frac{3 \cos^2 \theta^* - 1}{2}, \quad d_{21} = -\sqrt{\frac{3}{2}} \sin 2\theta^* \cos \phi^*, \quad d_{22} = \sqrt{\frac{3}{2}} \sin^2 \theta^* \cos 2\phi^*,$$

with σ_0 the unpolarized cross section, T_{2i} the tensor analyzing powers, and P_{zz} the degree of tensor polarization. The polarization axis of the deuteron is defined by the angles θ^* and ϕ^* in the frame where the z axis is along the direction of the three-momentum transfer \vec{q} and the x axis is perpendicular to z in the scattering plane.

The experiment was performed using a 704 MeV electron beam in the AmPS storage ring [8] and a tensor-polarized deuterium internal target [9] at NIKHEF (Amsterdam). By stacking several pulses of electrons, produced by the medium-energy accelerator, circulating currents of up to 150 mA were stored in the ring. A beam

lifetime in excess of 2000 s was obtained by compensating synchrotron radiation losses with a 476 MHz cavity.

Nuclear-polarized deuterium gas was provided by an atomic beam source. Deuterium atoms are produced by means of an rf dissociator. Atoms with their electron spin up are focused into the target-cell feed tube by two sextupole magnets, whereas those with spin down are defocused. A medium- and a strong-field rf unit induce transitions between the hyperfine states, resulting in a tensor polarization P_{zz}^- (P_{zz}^+) of ideally -2 ($+1$) with zero vector polarization. The tensor polarization was flipped every 20 s between P_{zz}^- and P_{zz}^+ . The atomic

beam is fed into an open-ended T-shaped dwell cell with a diameter of 15 mm and a length of 400 mm. The cell was cooled to approximately 150 K. With a flux of 1.3×10^{16} atoms/s in two hyperfine states into the cell an integrated target density was obtained of 2×10^{13} atoms/cm². The direction of the deuteron polarization axis was defined by a magnetic holding field ($B = 23$ mT) and chosen to be on average parallel to the three-momentum transfer (at $\approx 62^\circ$ to the beam direction).

Two polarimeters were available to study the polarization in the dwell cell. A small sample (10%) of the atomic beam was continuously analyzed by a Breit-Rabi polarimeter. The nuclear polarization of the atoms and the composition of the gas in the dwell cell was measured with an ion-extraction system [10]. Ions, produced by the circulating electrons, were extracted from the beam line and transported through a Wien filter (an $E \times B$ velocity selector). Since molecular and atomic deuterium ions have different velocities, measuring the ion current as a function of the Wien filter B field allows determination of the atomic fraction averaged over the target cell. The nuclear polarization can be determined by accelerating the ions onto a tritium target and using the well-known analyzing power [11] of the low-energy reaction ${}^3\text{H}({}^2\text{H}, n)\alpha$. We measured the polarization of molecules, originating from recombination in the cell, in a dedicated experiment [12]. Combining these measurements the effective target polarization was determined to be $\Delta P_{zz} = P_{zz}^+ - P_{zz}^- = 1.175 \pm 0.057$.

The scattered electrons were detected in an electromagnetic calorimeter [13] consisting of 6 layers of CsI(Tl) crystals with a total depth of 19 radiation lengths. The first layer of CsI(Tl) was sandwiched between two plastic scintillators. The second of these, shielded from low-energy Møller electrons, provided the trigger. A pair of wire chambers provides tracking information of the detected electrons. The calorimeter, with an acceptance of approximately 150 msr, was positioned at a central angle θ_e of 45° .

The ejected or recoiling hadrons were detected in coincidence in a so-called range telescope (RT) [14], consisting of 16 layers of plastic scintillator. The first layer had a thickness of 2 mm, all following layers were 10 mm thick. This detector was also preceded by two wire chambers, and was positioned at a central angle of 62.3° . The kinetic energy of the recoiling deuterons was kinematically limited to 120 MeV.

Event selection was based on coincidence timing between the two arms, the response of the RT scintillators and on tracking information. The coincidence time was corrected for effects from walk, time of flight, and impact position on the trigger scintillators.

Particle identification was performed by comparing the response of the RT scintillators to the energy loss, calculated using the formula of Bethe and Bloch [15]. A particle identification parameter P_{id} was defined as

$$P_{id} = \frac{1}{N} \sum_{i=1}^N \frac{\mathcal{L}_{meas}}{\mathcal{L}_{calc}} \quad (2)$$

with N the number of active RT scintillators and \mathcal{L}_{meas} (\mathcal{L}_{calc}) the actual (calculated) response in the i th scintillator. P_{id} will display a peak around 1 for deuterons, and a peak at smaller values for protons and electrons.

For the kinematically overdetermined elastic scattering reaction, requiring correlations between the scattering angles of the electron and the hadron reduces the number of protons even further.

Figure 1 shows the distribution of P_{id} and the coincidence timing τ_p between the scattered electron and the recoiling hadron. To obtain this distribution $\pm 2.5\sigma$ cuts were applied on their angular correlations. A clear separation is observed between protons and deuterons. The proton contamination was estimated to be 4.6%. Analysis of a proton sample has shown that these have an analyzing power much lower than that of the deuterons. Scattering from the cell walls was observed to be negligibly small in runs without gas flowing into the cell.

In the event selection additional $\pm 2.5\sigma$ cuts were applied on the coincidence time and on P_{id} . An asymmetry A_d^T was formed for events that fall within a 0.5 fm^{-1} wide Q bin, using the expression

$$A_d^T = \sqrt{2} \frac{N^+ - N^-}{P_{zz}^+ N^- - P_{zz}^- N^+} \quad (3)$$

with N^+ (N^-) the number of events in the Q bin considered when the target polarization was positive (negative). To correct for the fact that the direction of the holding field—and thus the spin orientation—varies over the length of the cell with respect to \vec{q} the uncorrected tensor asymmetry A_d^T is weighted with d_{20} from Eq. (1).

Note from Eq. (1) that A_d^T contains small contributions from T_{21} and T_{22} . Since A_d^T can be expressed as a function of T_{20} , A and B , one can derive T_{20} from A_d^T using the world data set for the unpolarized structure functions

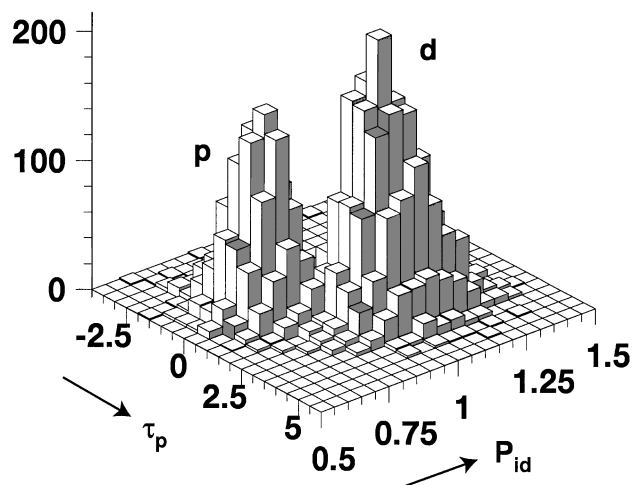


FIG. 1. Particle identification parameter P_{id} (defined in the text) versus coincidence time τ_p .

TABLE I. Result on A_d^T , $T_{20}(70^\circ)$, and G_C with statistical and systematic uncertainties, extracted from our T_{20} measurements and the world data on A and B .

Q [fm^{-1}]	A_d^T	$T_{20}(70^\circ)$ (stat.)	(syst.)	G_C (stat.)	(syst.)
2.03	-0.683	-0.713(0.082)	(0.036)	0.163(0.003)	(0.014)
2.35	-0.891	-0.897(0.081)	(0.045)	0.100(0.003)	(0.009)
2.79	-1.383	-1.334(0.223)	(0.066)	0.035(0.015)	(0.005)

A and B (see [7] for an overview). To investigate the sensitivity of the extraction procedure to the uncertainty in the input parameters (i.e., Q , θ_e , d_{2i} , A_d^T , A , and B), these were varied independently within their error and the extraction repeated. The total error was taken to be the quadratic sum of the separate errors. Note that the main contribution to the systematic error in A_d^T comes from the systematic uncertainty in the polarization.

The observables A , B , and T_{20} provide three different combinations of the form factors G_C , G_Q , and G_M , from which these can be extracted. The result for T_{20} was recalculated at $\theta_e = 70^\circ$, to allow a direct comparison with the results of other experiments. The extracted values for T_{20} and G_C are shown in Table I and in Fig. 2. The new data on T_{20} are each at least one σ below the predictions of nonrelativistic [1,2] and relativistic models [3,4]. This confirms the findings of the previous NIKHEF experiment [16].

To evaluate the model sensitivity of the T_{20} and t_{20} data sets a χ^2 analysis was performed, for which the data measured most recently at Bates [7], using a calibrated recoil parameter, and those from the NIKHEF experiments were selected. The data from BINP have poor accuracy at low Q [17] and poor discriminating power in the Q range from 1 to 3 fm^{-1} [18], since the T_{20} values were extracted by normalizing one datum to a selected model prediction. The selected data sets are compared to the calculations of Wiringa [1], Mosconi [2], Hummel [3], Van Orden [4], and Buchmann [20]. The first two calculations, both using the nonrelativistic impulse approximation, differ in the NN potential used (Argonne- v_{18} for Wiringa and Paris for Mosconi) and in the implementation of meson-exchange contributions. The Buchmann calculation used a nonrelativistic cluster model of constituent quarks and mesons in a limited parameter space, but fails to reproduce the data on A and B with great accuracy. The first two columns of Table II give the χ^2 values when only the T_{20} data of either experiment are considered. In addition, both these experiments yielded data on other tensor analyzing powers: in the 95 data run of NIKHEF [16] T_{22} was also determined, and the Bates experiment determined all tensor moments simultaneously. The last two columns of the table give the results when all data are taken into account.

The two data sets lead to different conclusions about the quality of the models. The NIKHEF set shows a preference for nonrelativistic calculations with realistic NN potentials, when only the T_{20} data are considered, and this conclusion remains unaltered when the datum on T_{22} is included in the fit. The Bates data set, on the other

hand, shows a preference for the relativistic calculations, but loses most of its discriminating power when all data on t_{2i} are taken into account, mainly due to an inconsistency in one value of t_{22} . The then available data on T_{20} and t_{20} led Henning *et al.* [21] to point out an inconsistency in the location of the minimum of the charge form factor of two- and three-nucleon systems.

Stringent constraints are imposed on models by the extensive data for the unpolarized structure functions A and B , in addition to the polarized data. In Table III the result of a χ^2 -analysis is given for A and for B ,

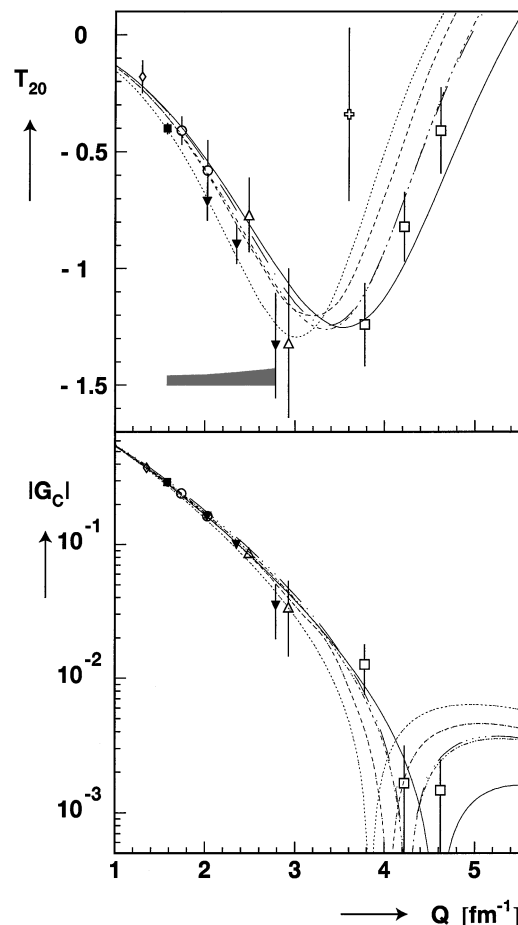


FIG. 2. Extracted values (solid triangles) of $T_{20}(70^\circ)$ (top) and G_C (bottom) as a function of Q compared to the world data and selected calculations. Data: solid triangles (present experiment), open squares [7], solid square [16], open diamond [17], open triangles [18], open circles [19], and open cross [6]. Curves: short-dashed [1], dash-dotted [2], full [3], long-dashed [4], dotted [20]. The shaded area indicates the size of the systematic errors from the present experiment.

TABLE II. χ^2/N analysis for NIKHEF (N95 + N96): [16] and present results) T_{2i} and Bates (B90: [7]) t_{2i} data, against various model predictions. N is the number of data points used in the analysis.

	$T_{20}(\text{N95} + 96)$ $N = 4$	$t_{20}(\text{B90})$ $N = 3$	$T_{2i}(\text{N95} + 96)$ $N = 5$	$t_{2i}(\text{B90})$ $N = 9$
Wiringa	1.14	2.40	1.37	3.35
Mosconi	1.31	0.30	1.48	2.46
Hummel	2.80	0.89	2.68	2.54
Van Orden	2.28	0.29	2.27	2.52
Buchmann	0.16	5.15	0.57	3.32

together with the overall χ^2 . Data [7] for A and B in the Q range of 0.5 to 6.0 fm^{-1} were taken into account. The normalization of each data set was varied within the quoted systematic uncertainty until a minimum value for the χ^2 was obtained. The best description is given by the nonrelativistic calculation of Ref. [1] that includes the relevant corrections to the impulse approximation, which conforms to the conclusions from the NIKHEF data. It should be noted that especially the inclusion of meson-exchange currents is of great importance, in describing both the unpolarized and the polarized data.

In conclusion, absolute measurements of the tensor analyzing power T_{20} were performed in a Q range from 1.8 to 3.2 fm^{-1} . This new data set, together with that of a previous measurement at NIKHEF, has provided additional stringent constraints on the deuteron form factors. Recently, an experiment [22] has been completed at Jefferson Laboratory, which will provide accurate data on t_{20} in a Q range from 4 to 6.5 fm^{-1} , thus covering the expected position [21] of the minimum in G_C . Future measurements of T_{20} are to be expected with the BLAST [23] detector at MIT-Bates in a Q range of 0.2 to 4.6 fm^{-1} .

This work was supported in part by the Stichting voor Fundamenteel Onderzoek der Materie (FOM), which is financially supported by the Nederlandse Organisatie voor Wetenschappelijk Onderzoek (NWO), the Swiss National Foundation, the National Science Foundation under Grants No. PHY-9316221 (Wisconsin), No. PHY-9200435 (Arizona State), and No. HRD-9154080 (Hampton), NWO Grant No. 713-119, and HCM Grants No. ERBCHBICT-930606 and No. ERB4001GT931472.

TABLE III. χ^2/N analysis of the A and B world data set.

Model	A $N = 81$	B $N = 34$	$A + B$ $N = 115$
Wiringa	5.6	5.9	5.7
Mosconi	11.0	1.8	8.3
Hummel	16.5	4.9	13.1
Van Orden	72.7	2.7	52.0
Buchmann	50.8	6.9	37.8

- [1] R. B. Wiringa, V. G. J. Stoks, and R. Schiavilla, Phys. Rev. C **51**, 38 (1995).
- [2] B. Mosconi and P. Ricci, Few-Body Syst. **6**, 63 (1989); **8**, 159(E) (1990); (private communication).
- [3] E. Hummel and J. A. Tjon, Phys. Rev. C **42**, 423 (1990).
- [4] J. W. Van Orden, N. Devine, and F. Gross, Phys. Rev. Lett. **75**, 4369 (1995).
- [5] T. W. Donnelly and A. S. Raskin, Ann. Phys. (N.Y.) **169**, 247 (1986).
- [6] S. G. Popov *et al.*, in *Proceedings of the 8th International Symposium on Polarization Phenomena in Nuclear Physics*, edited by E. J. Stephenson and S. E. Vigdor (Indiana University, Bloomington, Indiana, 1994), p. 530.
- [7] M. Garçon *et al.*, Phys. Rev. C **49**, 2516 (1994), and references cited therein.
- [8] G. Luijckx and R. Maas, in *Proceedings of the Fifth European Particle Accelerator Conference, EPAC96*, edited by S. Myers *et al.* (IOP, Bristol, 1996), p. 457.
- [9] Z.-L. Zhou *et al.*, Nucl. Instrum. Methods Phys. Res., Sect. A **405**, 165 (1998); Z.-L. Zhou *et al.*, Nucl. Instrum. Methods Phys. Res., Sect. A **378**, 40 (1996).
- [10] Z.-L. Zhou *et al.*, Nucl. Instrum. Methods Phys. Res., Sect. A **379**, 212 (1996).
- [11] J. W. van Ohlsen *et al.*, in *Proceedings of the 3rd International Symposium on Polarization Phenomena in Nuclear Reactions*, edited by H. H. Barschall and W. Haeberli (University of Wisconsin Press, Madison, Wisconsin, 1971), p. 503.
- [12] J. F. J. van den Brand *et al.*, Phys. Rev. Lett. **78**, 1235 (1997).
- [13] E. Passchier *et al.*, Nucl. Instrum. Methods Phys. Res., Sect. A **387**, 471 (1997).
- [14] H. B. van den Brink *et al.*, Nucl. Phys. **A587**, 657 (1995).
- [15] W. R. Leo, *Techniques for Nuclear and Particle Physics Experiments* (Springer-Verlag, Berlin, 1987).
- [16] M. Ferro-Luzzi *et al.*, Phys. Rev. Lett. **77**, 2630 (1996).
- [17] V. F. Dmitriev *et al.*, Phys. Lett. **157B**, 143 (1985).
- [18] R. Gilman *et al.*, Phys. Rev. Lett. **65**, 1733 (1990).
- [19] M. E. Schulze *et al.*, Phys. Rev. Lett. **52**, 597 (1984).
- [20] A. Buchmann, Y. Yamauchi, and Amand Faessler, Nucl. Phys. **A496**, 621 (1989).
- [21] H. Henning, J. Adam, Jr., P. U. Sauer, and A. Stadler, Phys. Rev. C **52**, R471 (1995).
- [22] S. Kox and E. Beise, JLab proposal E94-018.
- [23] Bates Large Acceptance Spectrometer Toroid, Technical Design Report, <http://mitbates.mit.edu/blast>